Fault measurement detection in a urban water supply network

José Ragot, Didier Maquin

Fault measurement detection in an urban water supply network

José Ragot *, Didier Maquin

Centre de Recherche en Automatique de Nancy, CNRS UMR 7039, Institut National Polytechnique de Lorraine, 2, Avenue de la forêt de Haye, 54516 Vandœuvre-les-Nancy Cedex, France

Abstract

For the improvement of the performance of technical processes, faults and abnormal system operation must be detected and identified. For that purpose different approaches for fault detection have been developed and, here, a model-based approach is used. A diagnosis strategy based on fuzzy residual analysis is presented in this paper. The proposed approach uses the analytical redundancy to detect and isolate faults on sensors. After a presentation of its principle, the method is applied to an urban water supply network. Thanks to the use of fuzzy concept, the suggested diagnosis procedure enables to take into account all the available data and knowledge. Moreover, its efficiency has been proved by using experimental data. Therefore, a supervision software has been developed on the basis of this fuzzy-based fault isolation method.

Keywords: Diagnosis; Fuzzy-based supervision; Fault isolation; Water supply network

1. Introduction

Supervision becomes an important interest centre for the managers of water supply networks [23,37]. They need to detect quickly all the unexpected events that could occur on the networks, such as leakage, damage or sensor bias. Indeed, the cost of water is increasing, so the loss of water must be reduced and the damages caused by leaks are often expensive. Moreover, the interruptions of water distribution are less and less tolerated by the consumers and 0particularly by industrialists. In other words, the safety and the reliability of water distribution networks must be improved. In this paper, the benefits of a model-based diagnosis for the safety and the reliability of water distribution networks is put into relief.

The organisation of a general model-based diagnosis procedure has been described in [9,12,21,34,1,29]. The first stage of the proposed procedure is the generation of residuals, which are revealing of the consistency between the model corresponding to the normal functioning state and the measurements [16]. A residual is a signal generated from some computation based on measured variables. It is ideally zero in a fault-free case and different from zero, in a faulty case. The main idea behind the residual generation that utilises quantitative models is redundancy which is based either on massive redundancy (several sensors measure the same variable) or analytical redundancy (several variables are linked by a relationship). Theoretically, residuals are zero mean in a normal functioning state and different from zero when they are affected by a fault. Then, for the second stage, on the basis of the residuals analysis, faults can be detected and isolated. Indeed, the resulting residual Boolean "signatures" are analysed, mostly by simple comparison with standard patterns to draw a diagnosis inference. Finally, a diagnosis can be established and depending on this diagnosis, actions of reconfiguring or maintenance can be started.

Various diagnosis procedures based on this general principle have been proposed. In papers [12,21,15], the authors suggest a method based on a binary codification of the

* Corresponding author. Tel.: +33 383595682; fax: +33 383595644.
E-mail addresses: jose.ragot@ensem.inpl-nancy.fr, jragot@ensem.inpl-nancy.fr (J. Ragot), dmaquin@ensem.inpl-nancy.fr (D. Maquin).

residuals; this codification associates to the residuals the value 1 if it is affected by a fault and the value 0 otherwise. This method appears to be easy to implement but its efficiency can be discussed. To improve this approach [31] proposed a method called DMP (diagnostic model processor), based on the works of [24], in which the residual evaluation is more progressive. Data reconciliation strategies are used to adjust process measurements subjected to random errors by satisfying material and energy balance constraints [32,27]. For that purpose, when gross errors or biases corrupt the measurements, they have to be detected and removed from the raw data before reconciliation. Moreover, recent works deal with the problem of data reconciliation in the presence of gross errors [30].

More specially, in the field of water network distribution, paper [2] investigates the effects of imposing bounds on the measurements used in weighted least-squares (WLS) state estimation. In [28] a study of drinking water network yield was carried out in Paris in 2001 in order to analyse the consequences of the changes that took place during this period. In the field of network design, the work of [18] deals with a methodology based on a genetic algorithm that has been developed for lower cost design of new and augmentation of existing water distribution networks. In [25], a model-based estimation process is simulated in order to determine leaks in a water transmission line. In [14], the authors design a neural network allowing the state estimation of a water distribution system including the determination of a confidence interval for each flow-rate. More generally there are a lot of works in the field of water network processing including design [6,11,36], modeling, control [35], optimisation [11,23], sensor positioning [3,20], simulation [13], leak detection [25,7,22,8].

A model-based fault isolation procedure using fuzzy concepts is described in this paper. To begin with, the general principle of the fuzzy-based fault isolation procedure is explained and illustrated with an academic example. Then, in order to improve the efficiency of the fault isolation some extensions of the method are proposed. The following section concerns an application of the fuzzy-based approach to an urban water supply network. Finally, some concluding remarks and prospects are presented in the last section.

2. Fault detection and isolation

2.1. Principle of the method

The basic idea behind model-based fault detection and isolation is to check whether measurements exhibit the behaviour corresponding to a model of the process in a normal working mode. When a change from a normal mode is detected, methods using distance measurements between data and models can be used for fault isolation. As previously mentioned, model-based FDI encompasses two main steps: generation of residuals and decision [4,16]. The latter itself may be split up in a stage of fault detection and a stage concerning fault isolation (or localisation). Most of the FDI techniques use parity functions to generate residuals; a parity function is an algebraic or a differential relationship based on a model process and observed measurements such that the measurement noise can be neglected. In the absence of fault, the residual is zero and when a fault occurs the residual takes a nonzero value.

For example, let us consider at time k the following set of $n = 4$ residuals that link $v = 5$ measurements:

$$\begin{cases} r_1(k) = f_1(x_1(k), x_2(k), x_5(k)) \\ r_2(k) = f_2(x_1(k), x_3(k)) \\ r_3(k) = f_4(x_1(k), x_2(k), x_3(k)) \\ r_4(k) = f_4(x_2(k), x_3(k), x_4(k)) \end{cases} \quad (1)$$

The theoretical matrix of fault signature, Σ, is defined by coding with binary variables the occurrence of variables in the different residuals r_i. Analysing Σ shows that for each fault to be detectable, no column of Σ should contain only zero elements and for each signature to be unique all the columns must be different. For the considered example, we have the following definition ("X" indicates that the fault in the corresponding column affects the residual of the corresponding row, "0" is used in other cases):

$$\Sigma = \begin{pmatrix} X & X & 0 & 0 & X \\ X & 0 & X & 0 & 0 \\ X & X & X & 0 & 0 \\ 0 & X & X & X & 0 \end{pmatrix} \quad (2)$$

This matrix expresses the theoretical influence of the faults onto the residuals. Indeed, to the jth column (signature) of Σ that will be denoted Σ_j, the jth fault may be associated. Then, the corresponding signature indicates how the fault affects the different residuals. A signature corresponding to a normal functioning may complete this matrix; this signature contains only null elements.

Statistical methods of abrupt change detection permit, at each sample time k, to code in a binary form $s_i(k)$ a set of experimental residuals $r_i(k)$, $i = 1, \ldots, n$ computed from the collected measurements:

$s_i(k) = 0$, if the taking into account of the value $r_i(k)$ in the analysis allows an abrupt change in $r_i(k)$ to be detected.
$s_i(k) = 1$, if this value does not allow an abrupt change in the residual $r_i(k)$ to be detected.

In this way, one builds the experimental signature $S(k) = (s_1(k) \cdots s_n(k))^{\mathrm{T}}$. The fault localisation is then obtained by searching, in the theoretical signature matrix Σ, that corresponds to the observed experimental signature. For example, the signature $S(k) = (1 \quad 0 \quad 0 \quad 0)$ corresponds to the fifth fault.

In practice, due to the influence of the noise, the experimental signatures are often degraded. The most frequent

situation is the transformation of a 1 into a 0 corresponding to a non-detection. For example, the experimental signature $S(k) = (1 \quad 0 \quad 1 \quad 0)$ does not exist in Σ, probably due to a fault of insufficient magnitude); however, the signature is not too far from the second column of Σ which corresponds to the second fault signature. This situation has been extensively studied by [17,16,4]. Indeed, according to the residual sensitivity to certain faults (this sensitivity does not intervene in the proposed coding), certain small magnitude faults cannot been detected by the proposed statistical tests. The localisation must therefore been done with the help of a distance calculus between the experimental and theoretical signatures. The most probable fault is that corresponding to the theoretical signature closer to the experimental one. The most frequently employed signature is the Euclidian one, defined by the distance between the experimental signature and each theoretical signature:

$$d_j(k) = \left(\sum_{i=1}^{n} \left(\Sigma_{ij} - s_i(k) \right)^2 \right)^{1/2} \qquad j = 1, \ldots, v \tag{3}$$

(s_i and Σ_{ij} being the components of s and Σ).

The performance of this recognition step depends on the dissimilarity of the theoretical signatures. In the vector space $\{0,1\}$, the points representing the binary vectors of signatures must be as distant as possible [17]. The goal of the structuration of residuals is precisely to increase the distances between the different theoretical signatures. Indeed, facing with r decision errors when analysing the experimental residuals, we need a Hamming distance equal to at least to $2r+1$ to guarantee the correct localisation of a fault.

More information may also be kept by using a ternary coding of the residuals that take into account the sign of the detected abrupt change. In this case, we have: $s_i(k) = 1$, if the detected abrupt change in the residual r_i is positive, $s_i(k) = -1$, if the detected abrupt change in the residual r_i is negative $s_i(k) = 0$, if no abrupt change in the residual is detected r_i is zero.

A similar analysis to those previously presented allows the fault to be detected.

For example, let us consider residuals (1) with supplementary information about the signs of the derivatives $\partial f_i / \partial x_j$ which are collected in the matrix S_g:

$$S_g = \begin{pmatrix} >0 & >0 & 0 & 0 & <0 \\ <0 & 0 & >0 & 0 & 0 \\ >0 & >0 & <0 & 0 & 0 \\ 0 & >0 & >0 & >0 & 0 \end{pmatrix} \tag{4}$$

Thus, two signature tables (Tables 1 and 2) can be established, according to the sign of the effects of the faults on the residuals.

Then, if for example x_1 is corrupted by a negative fault (the value of x_1 is less than the true value), then the residual signature is $(+1 \quad -1 \quad +1 \quad 0)^T$; i.e. the fault induces a positive deviation of the first and the third residuals, a negative one of the second and does not influence the fourth residual. Fault isolation consists in solving the reverse problem; from the residual values we need to deduce what the faults are. For that purpose, a rule-base linking symptoms is elaborated. Fuzzy rules are linguistic *IF–THEN* constructions that have the general form *IF A THEN B* where A and B are (collections of) propositions containing linguistic variables. A is called the premise and B is the consequence of the rule. In effect, the use of linguistic variables and fuzzy *IF–THEN* rules exploits the tolerance for imprecision and uncertainty. In this respect, fuzzy logic mimics the crucial ability of the human mind to summarise data and focus on decision-relevant information. Each rule is made up of a premise part related to a fault. For example, (see Table 2), from the previous signature matrix and for the fault f_1^-, one can write the rule:

if $r_1(k)$ is positive and $r_2(k)$ is negative and
$r_3(k)$ is negative and $r_4(k)$ is null then the fault
f_1^- is present (5)

Table 1
List of symbols

f	Fault
f^+, f^-	Positive or negative fault
h	Height
k	Discrete time
M	Incidence matrix
m_{ij}	Incidence matrix terms
μ	Membership function
μ^-	Membership function for negative modality
μ^0	Membership function for zero modality
μ^+	Membership function for positive modality
p	Pressure
q	Flow-rate
r	Residual
Σ	Signature matrix
Σ^-, Σ^+	Negative and positive signature matrices
S	Tank section
τ	Threshold
w	Pumping state
x	State variable
y	Measurement
ϵ	Measurement error
d	Distance between two signatures

Table 2
S^-: rule-base used for negative fault isolation

	f_1^-	f_2^-	f_3^-	f_4^-	f_5^-
r_1	+1	+1	0	0	−1
r_2	−1	0	+1	0	0
r_3	+1	+1	−1	0	0
r_4	0	+1	+1	+1	0

2.2. Fuzzy-based fault detection and isolation

The method presented in this paragraph uses a non-Boolean inference technique and is based on elementary notions related to fuzzy set theory. A fuzzy set is characterised by a membership function expressing the progressive

character of the transition between "belonging" and "not belonging". It is then defined by

$$A = \{(x, \mu_A(x)) | x \in X\} \tag{6}$$

where $\mu_A(x)$ represents the membership function of the x element of the fuzzy set A defined on the definition support X and taking values in the interval $[0,1]$. Fuzzy sets can represent "linguistic variables" which express a qualitative or imprecise knowledge such that "the magnitude of the residual is great".

The suggested fault isolation method uses fuzzy concepts. This method relies upon the residuals fuzzification. For each residual, three fuzzy sets r_j^-, r_j^0 and r_j^+ are defined; they correspond to the modalities "$-$", "0" and "$+$" for "negative", "zero" and "positive". The fuzzy set r_j^0 corresponds to the case of consistency of the residual r_j, whereas r_j^- and r_j^+ correspond respectively to the case of negative and positive inconsistency. The membership functions μ_j^-, μ_j^0 and μ_j^+, respectively associated to the fuzzy sets r_j^-, r_j^0 and r_j^+, are defined by expressions (1). The shape of these membership functions appears in Fig. 1. Eq. (7) expresses a typical choice (with a hyperbolic tangent function):

$$\mu_j^-(r_j(k)) = \frac{1}{2}\left(1 + \tanh\frac{r_j(k) - \tau_j}{p}\right) \tag{7a}$$

$$\mu_j^+(r_j(k)) = \frac{1}{2}\left(1 - \tanh\frac{r_j(k) + \tau_j}{p}\right) \tag{7b}$$

$$\mu_j^0(r_j(k)) = 1 - \mu_j^-(k) - \mu_j^+(k) \tag{7c}$$

where k refers to the time, τ_j and $-\tau_j$ define the evolution area of residual r_j in normal functioning (τ is a form factor which defines the variation rate of the membership function), p is related to the slope of the membership function. So, for each residual r_j and at each time k, the value of the membership functions μ can be computed. The following vector can then be built for each residual $r_j(k)$:

$$\mu_j(r_j(k)) = \left(\mu_j^-(r_j(k)) \quad \mu_j^0(r_j(k)) \quad \mu_j^+(r_j(k))\right)^{\mathrm{T}} \tag{8}$$

Fault isolation is based, on the one hand, on the observation of the symptoms affecting the residuals and, on the other hand, on the analysis of the fault signature matrix.

Let us consider, for instance, the fault f_1^- whose theoretical signature is (Table 2): r_1 positive, r_2 negative, r_3 positive and r_4 null. For the first residual r_1, this fault

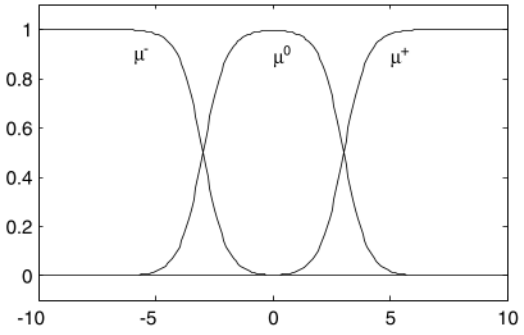

Fig. 1. Membership functions.

situation is characterised by a value of the membership function $\mu_{r_1}^+$ close to 1 and values of membership functions $\mu_{r_1}^0$ and $\mu_{r_1}^0$ close to 0. With regard to the other residuals, the values of the membership functions $\mu_{r_2}^-$, $\mu_{r_3}^+$ and $\mu_{r_4}^0$ are close to 1 whereas the values of the other membership functions are close to 0. Fault isolation consists in solving the reverse problem. That means deducing, from the value of the residual membership functions, the corresponding fault situation. So, for each fault situation a rule is established. Let us consider again the previous example, by calling f_1^- the envisaged fault situation. The rule corresponding to f_1^- is

$$\text{if } r_1(k) \text{ is } r_1^+ \text{ and } r_2(k) \text{ is } r_2^- \text{ and } r_2(k) \text{ is } r_3^+ \text{ and } r_4(k) \text{ is } r_4^0 \text{ then fault is } f_1^+ \tag{9}$$

where r^+, r^- and r^0 are the modalities "positive", "negative" and "zero". The quantification of proposition "is" is done by the means of membership grades of the residuals to these modalities. For example, the premise if $r_1(k)$ is r_1^+ is quantified by the value $\mu_{r_1}^+$ of the membership grade of $r_1(k)$ to r_1^-.

The symbol *and* appearing in this rule refers to a conjunction operator defined subsequently. In the same way a rule can be associated to each fault situation. A rule-base is then obtained. After that, the truth value μ_f of each rule is computed. To compute these values, aggregation operators must be defined. Various aggregation operators can be used [5]. The "minimum" (10), "mean" (11), "product" (12) operators are in current use:

$$\mu_f = \min\left(\mu_{r_1}^{A_1}, \ldots \mu_{r_p}^{A_p}\right) \tag{10}$$

$$\mu_f = \frac{1}{p}\sum_{i=1}^{p} \mu_{r_i}^{A_i} \tag{11}$$

$$\mu_f = \prod_{i=1}^{p} \mu_{r_i}^{A_i} \tag{12}$$

where $A_j \in \{-, 0, +\}$ according to the influence of f on r_j. For example, with the previous example, using (10):

$$\mu_{f_1}^- = \min(\mu_{r_1}^+, \mu_{r_2}^-, \mu_{r_3}^+, \mu_{r_4}^0) \tag{13}$$

Another useful operator (14) corresponding to a combination of the "mean" and "minimum" operators, is specifically defined for this problem of fault isolation. In particular, it increases the robustness of the proposed fault isolation method by handling separately the sensitive (negative or positive modality) and insensitive (zero residuals modality) truth values.

$$\mu_f = \min\left(\frac{1}{p}\sum_{i\in I_p} \mu_{r_i}^{A_i}, \frac{1}{q}\sum_{i\in I_q} \mu_{r_i}^{A_i}\right) \tag{14}$$

$$I_p = \{i | A_i \in \{0\}\}, \quad I_q = \{i | A_i \in \{-, +\}, \quad p = \mathrm{Card}(I_p), \quad q = \mathrm{Card}(I_q)$$

where $A_j \in \{-, 0, +\}$ according to the influence of f on r_j. The isolation result is based on the analysis of these truth

values. Indeed, the rule whose truth value is the highest designates the most likely fault hypothesis.

3. Example

To illustrate the principle of this method, an academic example is now presented; this example has the same formal structure as those used in Section 2.1. Let us consider a residual vector $r = (r_1 \quad r_2 \quad r_3 \quad r_4)^T$ defined by the following equation:

$$r = My \tag{15}$$

$$y = (y_1 \quad y_2 \quad y_3 \quad y_4 \quad y_5)^T$$

$$M = \begin{pmatrix} 1 & 8 & 0 & 0 & -1 \\ -1 & 0 & 2 & 0 & 0 \\ 2 & 1 & -5 & 0 & 0 \\ 0 & 1 & 1 & 2 & 0 \end{pmatrix}$$

3.1. Fault analysis

Let us consider the case of a positive bias (magnitude 0.75) affecting measurement y_1 from time 30 to time 60, a negative bias (magnitude 0.50) affecting measurement y_3 from time 90 to time 120 and a positive bias (magnitude 0.50) affecting measurement y_4 from time 150 to time 180. Evolution of measurements y_1 to y_5 on a horizon of 200 points is given in Fig. 2 (the dashed vertical lines indicate the intervals where data are biased).

For this example the fault signature matrices corresponding to faults affecting the measurements y_i, $i = 1, \ldots, 5$ are considered and a somewhat difficult situation is considered, i.e. the noise corrupting the measurement being important. The faults written f_i^- and f_i^+ designate respectively the case of negative and positive faults affecting measurement y_i. First of all, the fault signature matrices S^- and S^+ corresponding respectively to the negative (f_i^-) and positive (f_i^+) faults must be built. The matrices S^- and S^+ are then used for the generation of a rule-base. This rule-base is described by Tables 1 and 2 of Section 2.2.

Theoretically, referring to the signature matrix S^+, the fault situation f_1^+ should affect positively the residuals r_1 and r_3 and negatively the residual r_2 whereas r_4 is insensitive to that fault. That is hardly confirmed by Fig. 3, on which the residuals r_1, r_2, r_3 and r_4 computed by using the faulty measurement y_i, are represented: in particular, the sensitivity of residual r_1 to the fault f_1^+ is poor. For the fault f_3^-, residual r_1, r_2 and r_3 are respectively "zero", "negative" and "positive" in the time interval [90, 120]; that tallies with the theoretical signature of Table 3 but the situation is more ambiguous for residual r_4. For fault f_4^+, results depicted in Fig. 5 in time interval [150, 180] satisfy the theoretical signature of Table 4.

To cope with this difficulty, the next step concerns the residual fuzzification according to definition (7). The fuzzification of residual r_i is illustrated by Fig. 4. In particular, this figure shows that, from times 30 to 60, the value of the membership function $\mu_{r_3}^+$ is higher than the values of $\mu_{r_3}^-$ and $\mu_{r_3}^0$. That means that residual r_3 is considered to be affected by a positive deviation from times 30 to 60.

The truth value evolution of failure hypothesis f_1^-, f_1^+, f_2^-, f_2^+, f_3^-, f_3^+, f_4^-, f_4^+, f_5^- and f_5^+, obtained with definition

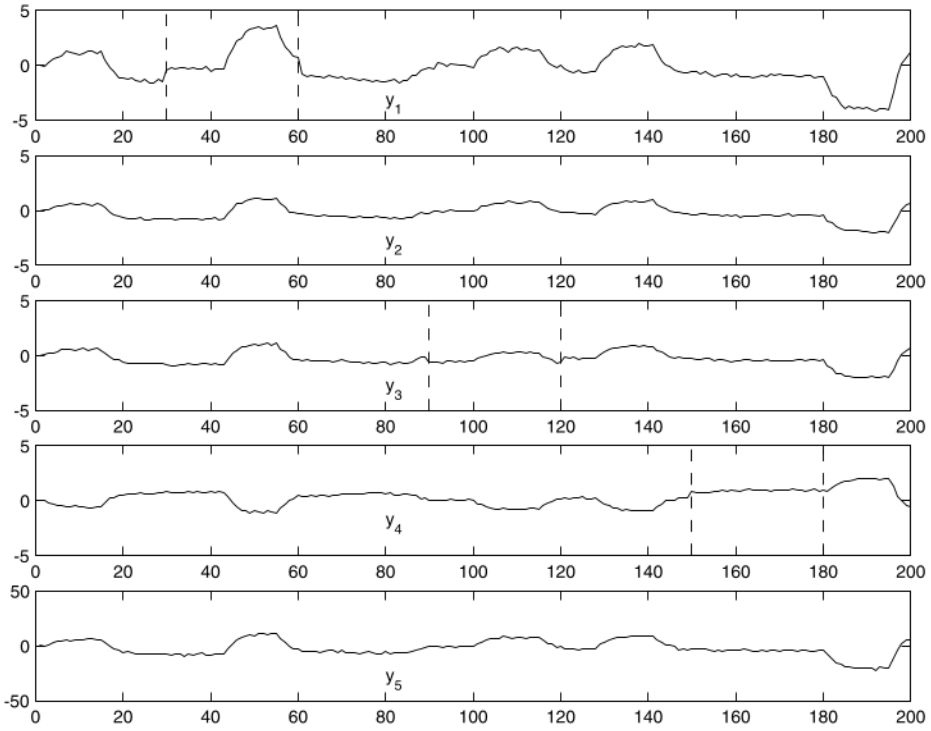

Fig. 2. Evolution of measurements y_1 to y_5.

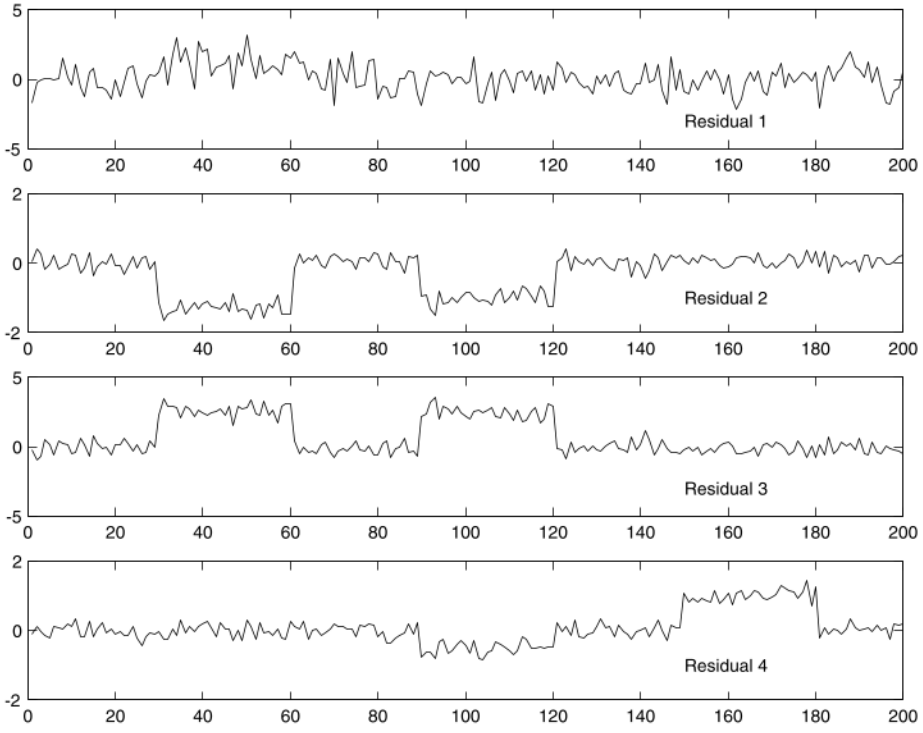

Fig. 3. Residuals r_1 to r_4.

Table 3
S^+: rule-base used for positive fault isolation

	f_1^+	f_2^+	f_3^+	f_4^+	f_5^+
r_1	−1	−1	0	0	+1
r_2	+1	0	−1	0	0
r_3	−1	−1	−1	0	0
r_4	0	−1	−1	+1	0

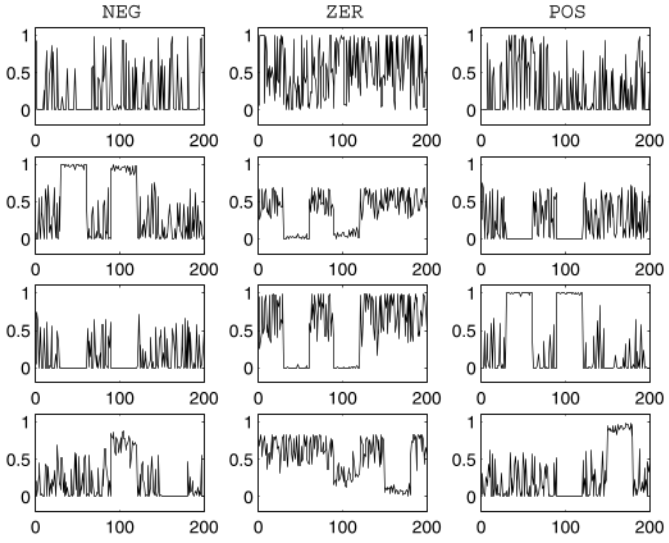

Fig. 4. Fuzzification of residuals r_1 to r_4.

(10) are shown in Fig. 5. The analysis of all the truth values leads to conclude that the most likely failure hypotheses are: f_1^+ approximately from time 100 to 120, f_3^- approximately from time 40 to 60 and f_4^+ approximately from time 160 to 180. That means that the positive fault affecting measurement y_3 is now isolated successfully.

Table 4
Fault signature ("X" is used to specified a fault affecting a residual)

Fault	r_1			r_2			r_3			r_4		
	r_1^-	r_1^0	r_1^+	r_2^-	r_2^0	r_2^+	r_3^-	r_3^0	r_3^+	r_4^-	r_4^0	r_4^+
f_1^-	X	·	·	·	·	X	X	·	·	·	X	·
f_1^+	·	·	X	X	·	·	·	·	X	·	X	·
f_2^-	X	·	·	·	X	·	X	·		X	·	·
f_2^+	·	·	X	·	X	·	·	·	X	·	·	X
f_3^-	·	X	·	X	·	·	·	·	X	X	·	·
f_3^+	·	X	·	·	·	X	X		·	·	·	X
f_4^-	·	X	·	·	X	·	·	X	·	X	·	·
f_4^+	·	X	·	·	X	·	·	X	·	·	·	X
f_5^-	·	·	X	·	X	·	·	X	·	·	X	·
f_5^+	X	·	·	·	X	·	·	X	·	·	X	·
None	·	X	·	·	X	·	·	X	·	·	X	·

3.2. Extensions of the method

3.2.1. Temporal persistence of the symptoms

Analysing the residual is somewhat difficult when noise influences these residuals. For example, fuzzified residual r_4^+ in Fig. 4 shows a lot of perturbations on time interval $[0,100]$ that are not due to a particular fault. In the approach presented previously, only the magnitude of the residuals is used to evaluate them. Consequently, a low truth value is systematically associated to faults which cause low deviations but the duration of these deviations

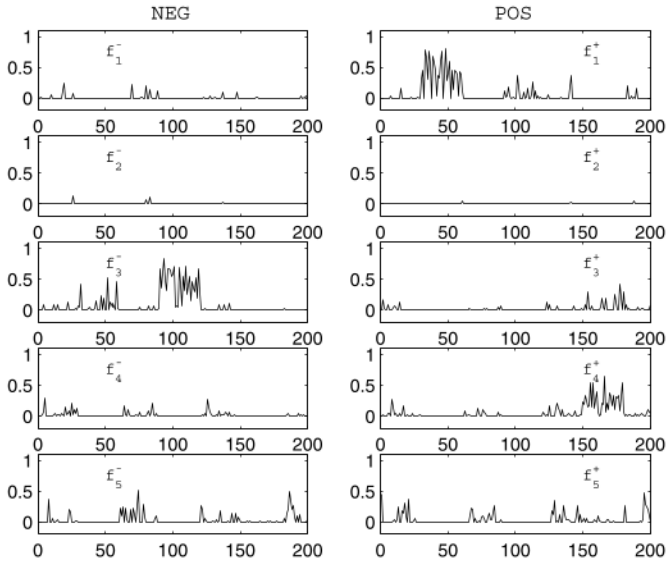

Fig. 5. Truth value of hypothesis f_1^-, f_1^+, f_2^-, f_2^+, f_3^-, f_3^+, f_4^-, f_4^+, f_5^- and f_5^+.

is not taken into account. Indeed, by taking into account the temporal persistence of the symptoms, low deviations can lead to high truth values, if the corresponding fault is persistent. So, by using an indicator of temporal persistence, the performance of this fault isolation procedure can be improved. Therefore, indicators of persistence p_j^-, p_j^0 and p_j^+ (16) are respectively associated to the membership functions $\mu_{r_j}^-$, $\mu_{r_j}^0$ and $\mu_{r_j}^+$ (7) of each residual. They correspond to the ratio of the number of values of the membership function higher than a given threshold S, $(0 < S < 1)$ on a sliding horizon of width L:

$$p_i^- = \frac{N(\mu_{r_j}^-)}{L} \quad j = (1, \ldots, L) \tag{16a}$$

$$p_i^0 = \frac{N(\mu_{r_j}^0)}{L} \quad j = (1, \ldots, L) \tag{16b}$$

$$p_i^+ = \frac{N(\mu_{r_j}^+)}{L} \quad j = (1, \ldots, L) \tag{16c}$$

with

$$N(\mu_{r_j}^-) = \mathrm{Card}(\mu_{r_j}^- : \mu_{r_j}^- > S) \tag{17a}$$

$$N(\mu_{r_j}^0) = \mathrm{Card}(\mu_{r_j}^0 : \mu_{r_j}^0 > S) \tag{17b}$$

$$N(\mu_{r_j}^+) = \mathrm{Card}(\mu_{r_j}^+ : \mu_{r_j}^+ > S) \tag{17c}$$

The quantities $N(\mu_{r_j}^-)$, $N(\mu_{r_j}^0)$ and $N(\mu_{r_j}^+)$ define respectively the number of membership function values of $\mu_{r_j}^-$, $\mu_{r_j}^-$ and $\mu_{r_j}^+$ which are higher than the threshold S on the considered sliding horizon L. Truth values (18) taking into account the residual membership values and the temporal persistence can then be computed:

$$\tilde{\mu}_{r_j}^- = \frac{1}{2}(p_j^- + \mu_{r_j}^-) \tag{18a}$$

$$\tilde{\mu}_{r_j}^0 = \frac{1}{2}(p_j^0 + \mu_{r_j}^0) \tag{18b}$$

$$\tilde{\mu}_{r_j}^+ = \frac{1}{2}\left(p_j^+ + \mu_{r_j}^+\right) \tag{18c}$$

The fault detection procedure is then similar to that described in Section 2.2 but by taking the values of $\tilde{\mu}$ instead of μ (18).

Consideration of temporal persistence is particularly interesting when the residual deviations are low and have to be reinforced according to the time. As an illustration, let us consider the residual appearing in (Fig. 6) which is affected by a positive deviation between time instants 70 to 200. Without taking into account the temporal persistence of the symptom the value of the membership function μ_r^+ (evaluated with (7b)) remains quite constant and does not reveal clearly the deviation of the residual (middle part of the figure). On the contrary, by taking into account the persistence of the symptoms, the value of the membership function (evaluated with (7b), (16c) and (18c)) grows clearly when the fault appears. To be honest with the reader, detecting a deviation in a residual strongly depends on several parameters and mainly: on one hand τ and p for the shape of the membership function (7) and, on the other hand, L and S for the persistency characterisation (16) and (17).

3.2.2. Notion of confidence

In some cases the confidence attached to the different analytical redundancy relations, used to generate the residuals are not identical. For example, redundancy relations describing material balances, which are theoretically exact, are often more reliable than relations based on a statistical analysis of the measurements. To take into account this difference, weights representative of the confidence can be introduced. Practically, a weight c_j (whose value is included between 0 and 1) is associated to each residual r_j, according to the confidence attached to the corresponding redundancy relation. The operators defined by expression (11), (12) and (14) are then used to compute the truth value of the failure hypothesis, by replacing the truth values by weighted truth values. The weights c_j are affected to the membership functions μ_{r_j}, as follows:

$$\mu_f = \frac{\sum_{i=1}^{p} c_j \mu_{r_i}^{A_i}}{\sum_{i=1}^{p} c_j} \tag{19}$$

$$\mu_f = \prod_{i=1}^{p} \left(\mu_{r_i}^{A_i}\right)^{c_j} \tag{20}$$

$$\mu_f = \min\left(\frac{\sum_{j\in I_p} c_j \mu_{r_j}^{A_j}}{\sum_{j\in I_p} c_j}, \frac{\sum_{j\in I_q} c_j \mu_{r_j}^{A_j}}{\sum_{j\in I_q} c_j}\right) \tag{21}$$

where the subsets I_p and I_q have been defined in (14).

3.2.3. Sensitivity to faults

Sensitivity to faults is a fundamental notion in the framework of fault isolation. Indeed, the sensitivities of residuals to a given fault situation are not identical. That means that the magnitude of the residual deviations can be used to characterise a fault situation. In other words, the difference of sensitivity can be exploited to improve the detectability and the isolability of the faults.

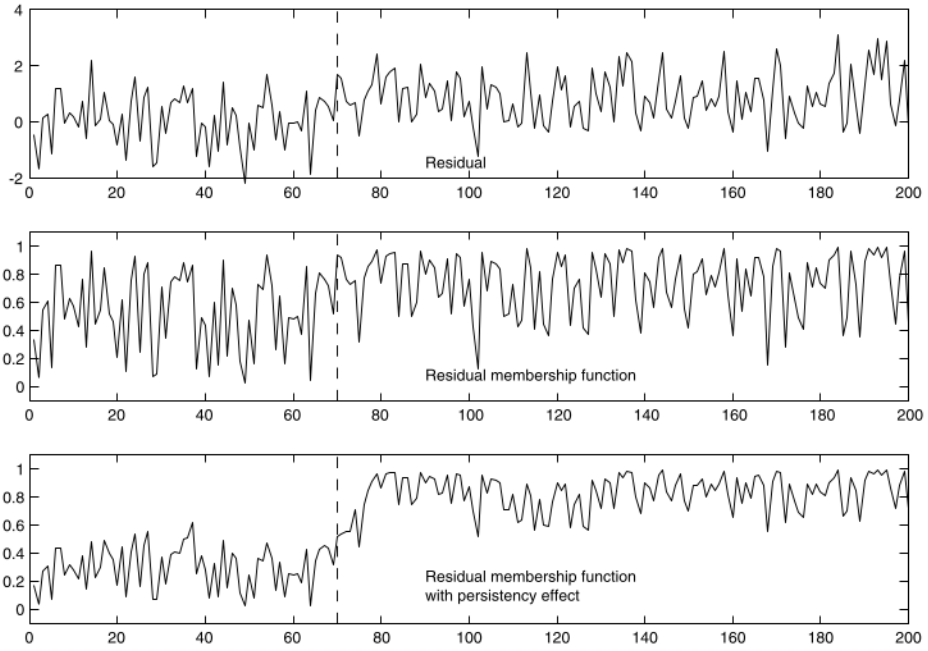

Fig. 6. Residual r affected by a low deviation at time 70, membership function without taking into account temporal persistence, membership function by taking into account temporal persistence.

First of all, it is important to analyse the relative contributions of the noise and the fault on residual values. For that purpose, let us express the measurement of a variable as the sum of the true value x (which is unknown), the noise ϵ which is generally assumed to be centred and random and the fault f:

$$y = x + \epsilon + f$$

As the true value x fully satisfies the process model, the residual (15) may be expanded:

$$r = r_\epsilon + r_f \tag{22a}$$

$$r_\epsilon = M\epsilon \tag{22b}$$

$$r_f = Mf \tag{22c}$$

where r_ϵ and r_f are the respective contributions of the noise and the fault. Expression (22a) clearly shows that the effect of the fault f may be masked by those of the noise ϵ according to their relative magnitudes. In order to quantify this phenomena, let us consider in (22b) the expression of the ith residual:

$$r_{\epsilon,i} = \sum_{j=1}^{v} m_{ij}\epsilon_j \tag{23}$$

where m_{ij} are the entries of M. Let us accept the hypothesis of bounded measurement error and denoting e_j the bounds of ϵ_i allows to define the boundary τ_j of the residual:

$$r_{\epsilon,i} = \sum_{j=1}^{v} |m_{ij}|e_j \tag{24}$$

The bound has to be known from the precision of the measurement devices or to be selected by the user according to his knowledge of these devices (without any knowledge, it is always possible to select that bound proportional to the magnitude of the measurements). Then (24) expresses the upper bound of the contribution of the noise upon the residuals. According to (22c), the influence of a fault can also be quantified. Considering an unique fault f_j affecting the jth variable, its contribution to the ith residual is

$$r_{f,ij} = m_{ij}f_j \tag{25}$$

Comparing (24) and (25) defines the lowest magnitude fault allowing to separate the influences of the noise and of the fault in the residual. This bound is defined by

$$\tau_{ij} = \frac{\sum_{j=1}^{v} |m_{ij}|e_j}{|m_{ij}|} \tag{26}$$

Thus, the ith residual is sensitive to a fault on the jth stream, if the magnitude of that fault exceeds τ_{ij} (26). It should be noticed that, when $m_{ij} = 0$, this magnitude tends toward infinity. This is not totally surprising, since, in that case, variable j does not affect the residual.

The residual sensitivities must be quantified, and they naturally depend on the quantity τ_{ij} which is also called the (steady state) triggering limit [16]. Indeed, let us recall that τ_{ij} corresponds to the magnitude of fault f_i for which residual r_j is affected by a mean jump higher than a given threshold τ_{ij}. The values of the different thresholds are not very important but the same criteria must be used to set each of them, to be able to compare the values of terms τ_{ij}. From the values of τ_{ij}, weights δ_{ji}, representative of the normalised sensitivity of residual r_j to fault f_i are computed:

$$\delta_{ij} = \frac{1/\tau_{ij}}{\sum_{i=1}^{n} 1/\tau_{ij}} \tag{27}$$

In this way, high (resp. low) weights are associated to residuals which are highly (resp. lowly) sensitive to fault f_i. These weights are then used for the computation of the fault hypothesis truth values μ_{f_i}. As in previous section, the aggregation operator (7) is really suitable to take into account the weights δ_{ji}:

$$\mu_{f_i}(k) = \min\left\{\frac{\sum_{j\in I_p}\mu_{r_j}^{A_j(k)}}{|I_p|}, \frac{\sum_{j\in I_q}\mu_{r_j}^{A_j(k)}\delta_{ij}}{|I_q|}\right\} \tag{28}$$

where $A_j = \{-, 0, +\}$ according to the influence of f_i on r_j, $|E|$ designates the cardinal of subset E. Let us note that for the residuals on which the fault has no influence (residuals r_j such that $A_j = 0$), the weights δ_{ji} are not used in expression (22).

Let us consider again the example of Section 2.2 in order to appreciate the values of terms d_{ji} and weights δ_{ji}. The constraint matrix M and the values of e are given below:

$$M = \begin{pmatrix} 1 & 8 & 0 & 0 & -1 \\ -1 & 0 & 2 & 0 & 0 \\ 2 & 1 & -5 & 0 & 0 \\ 0 & 1 & 1 & 2 & 0 \end{pmatrix}$$

$$e = (0.1 \quad 0.4 \quad 0.3 \quad 0.1 \quad 0.1)^{\mathrm{T}}$$

From the knowledge of M and e, the values of residual bounds τ_{ji} (26) and sensitivities δ_{ij} (27) can be deduced (Tables 5 and 6). For example, in Table 5, the column relative to τ_1 shows that the if fault f_1 occurs, residual r_3 will fire if the magnitude of the fault is greater that 0.80; moreover, the experimental signature of fault f_1 is identical to the theoretical signature only if the magnitude of the fault is greater than 3.40. Thus, these bounds are strongly connected to the sensitivity of the residual to a fault. It is clear that r_4 is not sensitive to f_1 and r_2 is the most sensitive residual. Thus, normalised inverse of these bounds, as explained with (27), is a good interpretation of the sensitivity.

Table 5
Residual bounds

	τ_1	τ_2	τ_3	τ_4	τ_5
r_1	3.40	0.425	∞	∞	3.40
r_2	0.50	∞	0.25	∞	∞
r_3	0.80	1.60	0.32	∞	∞
r_4	∞	0.80	0.80	0.40	∞

Table 6
Residual sensitivity

	δ_1	δ_2	δ_3	δ_4	δ_5
r_1	0.08	0.56	0.00	0.0	1.0
r_2	0.56	0.00	0.48	0.0	0.0
r_3	0.35	0.15	0.37	0.0	0.0
r_4	0.00	0.30	0.15	1.0	0.0

4. Application to an urban water supply network

In most water distribution networks, a large percentage of the water is lost in transit from treatment units to consumers. Typically around 25% of production is lost or unaccounted for; this is due to several causes but mainly leakages, false measurement errors, public usage such as fire-fighting, earthquakes [33] and sometime severely cold weather. The cost involved with the maintenance of water distribution networks justifies the emerging of supervisory control; for a decade, most cities have developed investigation and audits to determine the amount of water lost in the distribution system. A trend that has emerged is to install permanent measurement devices to get information about flow-rates, pressures and levels. It is reasonable to correlate decrease of pressure and leaks. More generally all the information collected on the network, including the aforementioned measures but also logical information such as pumping startup, may be used to increase the knowledge of the system functioning. In some cases, direct measurement for leak detection are used, such as aquaphones, geophones or ground microphones and also resistivity measurements [10]. As explained in the introduction section, one problem that is very common in metering is the limited use made of the obtained data due to measurement errors.

Efficient control of a water distribution system requires accurate information about its current operating state. Thus, due to measurement errors, a data processing is needed, the main objective being to detect the faulty measurements and, eventually, to correct them. Generally, the direct measurements of flow, pressure and levels are combined with mathematical models of the system in order to reconcile discrepancies between the measurements [19,13,26].

4.1. Process description

The process considered in this work is an urban water supply network; a water distribution system is the essential link between the water supply source and the consumer. This process is depicted schematically in Fig. 7 where the symbols • indicate the flow-rate measurements and where h_j denotes the measured height in water storage. The part of the water network considered in this study is the storage network. The function of this network consists in sharing out water reserves among the whole town with the help of pumping stations, before its distribution to the consumers. More precisely, the storage network is composed of pumping stations that make up a treelike network regrouping about 30 tanks. On account of its importance for the water distribution reliability, the managers pay a great attention to the supervision of the storage network.

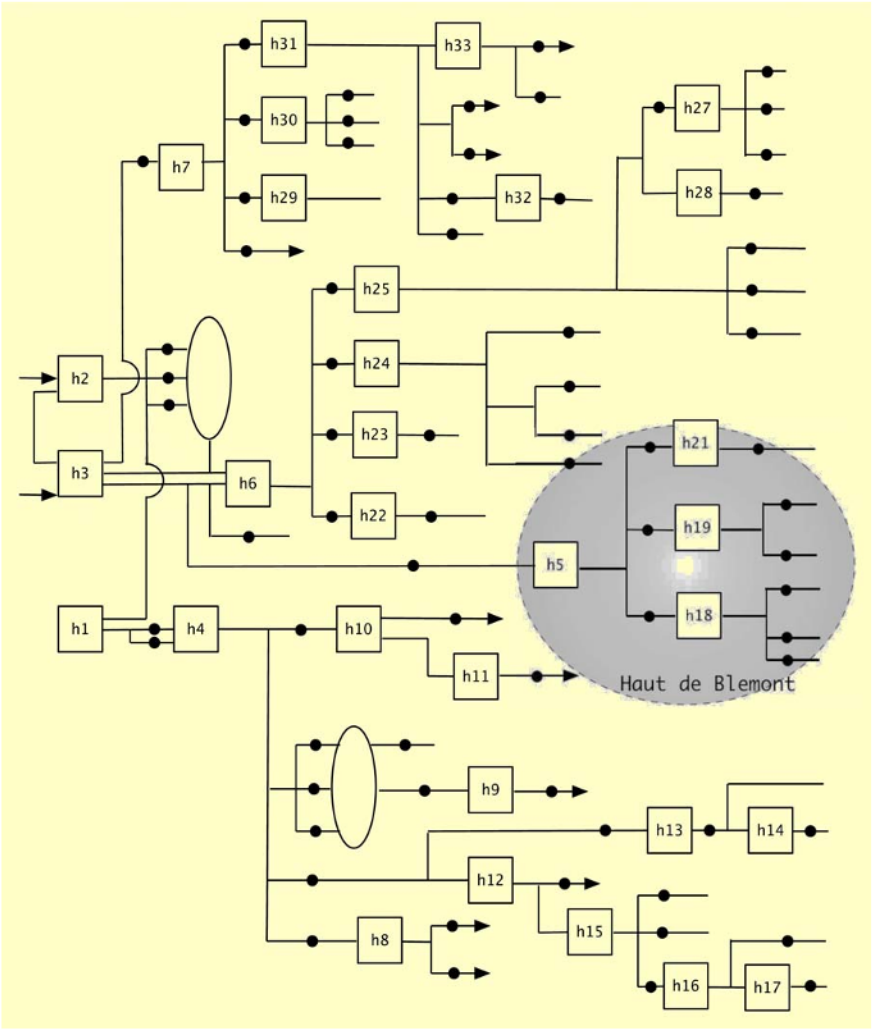

Fig. 7. Diagram of the water supply organisation.

Consequently, this part of the network has been supplied with numerous measuring devices. To each tank corresponds a water level measurement and roughly a hundred flow-rates are measured. About 30 pressure measurements are available as well and the data regarding the working state of each pump are collected. All in all, that represents roughly 200 sensors.

For the sake of clarity, the approach suggested in this paper is applied to only one of the pumping stations. But the extension to the whole network is practically immediate thanks to the use of a mathematical formalism.The considered pumping station, called "Haut de Blemont", is composed of four tanks. Its scheme appears in Fig. 8. The main tank called "Haut de Blemont" supplies, through pumps, three secondary tanks called "Albertin", "Haut de Ronces" and "La justice". Then, these tanks supply different areas of the town. For this pumping station the measurements collected are the water level (h_i) of the four tanks, ten flow rates (q_i) and the working state of the pumps (w_i). Besides, in the residence area supplied by flow-rate q_{44}, two pressures p_7 and p_8 are measured. The sampling period of these measurements is 1 min. As an example the experimental signals of measurements appear in Figs. 9 and 10.

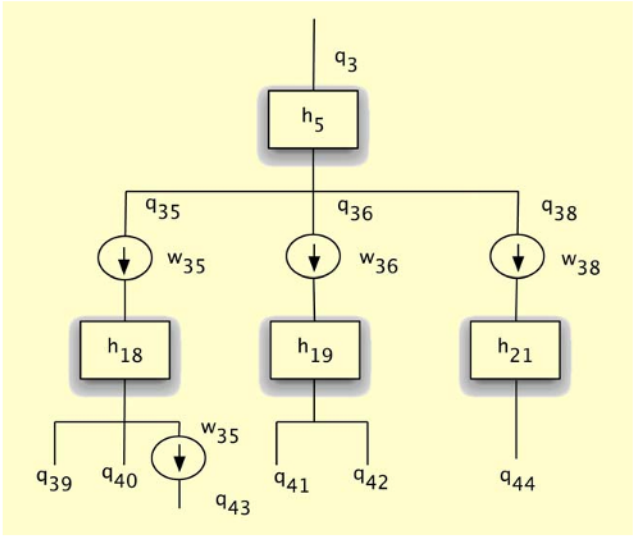

Fig. 8. Diagram of pumping station "Haut de Blemont".

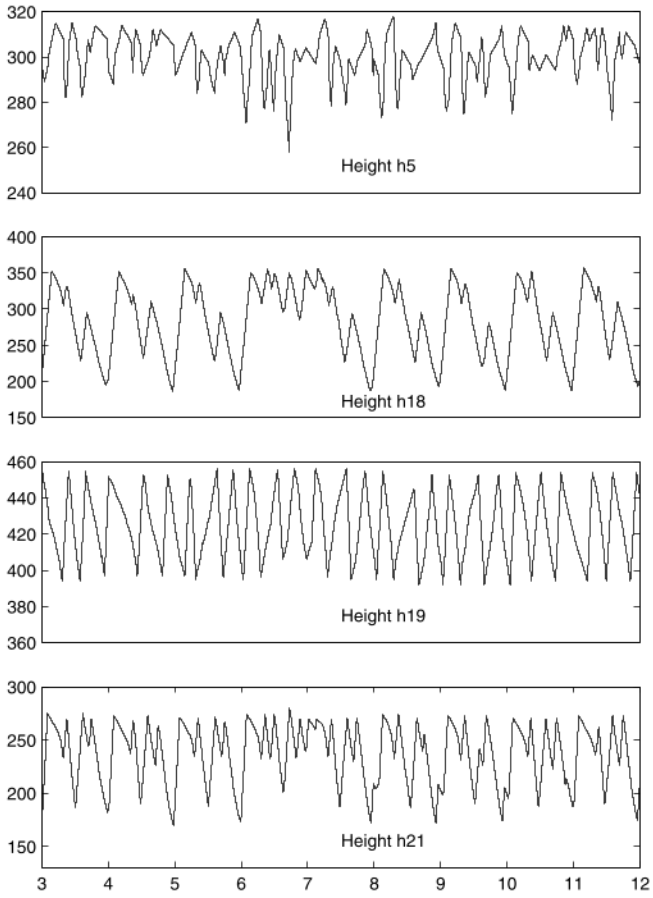

Fig. 9. Experimental signals: heights (cm).

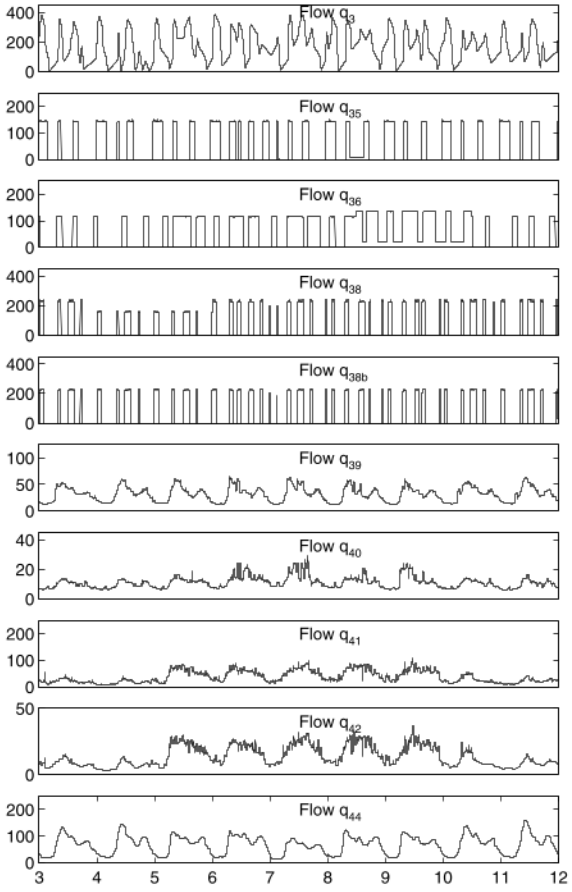

Fig. 10. Experimental signals: flow (m^3/h).

4.2. Analytical redundancy relations

After an analysis of the process and of the available data, different kinds of redundancy relations have been defined. They involve all the available information, namely flow-rates, pressures, pump working states and tank levels. These redundancy relations are presented more precisely in the next sections.

4.2.1. Material balance equations

The first kind of redundancy relations corresponds to material balance equations. For each tank a material balance equation can be written:

$$S_4 \frac{dh_4(t)}{dt} = q_3(t) - q_{35}(t) - q_{36}(t) - q_{38}(t) \quad (29a)$$

$$S_{18} \frac{dh_{18}(t)}{dt} = q_{35}(t) - q_{39}(t) - q_{40}(t) \quad (29b)$$

$$S_{19} \frac{dh_{19}(t)}{dt} = q_{36}(t) - q_{41}(t) - q_{42}(t) \quad (29c)$$

$$S_{21} \frac{dh_{21}(t)}{dt} = q_{38}(t) - q_{44}(t) \quad (29d)$$

where S_i, $i = 4, 18, 19, 21$ are the a prior known tank sections. Note that the flow q_{43} is omitted from (29b), the reason being the shut down of the corresponding pipe during our experiment on the true process. For numerical reasons, these equations may be converted into a discrete form involving the use of discrete measurements.

In the case of the pumping station "Haut de Blemont" this leads to four redundancy relations, one for each tank. A fifth relation can be established by comparing the measurements q_{38} and q_{38b} which correspond to the same flow-rate (material redundancy). Thus, q_{38} and q_{38b} are theoretically equal, which leads to redundancy relation (30):

$$q_{38}(k) - q_{38b}(k) = 0 \quad (30)$$

4.2.2. Use of pump working states

The working state of the pumps are useful for the generation of residuals too. The working state of the pumps delivering outflows q_{35}, q_{36} and q_{38} are respectively called w_{35}, w_{36} and w_{38}; Fig. 11 shows the evolution of the pump signals. The signals w_i are binary signals whose value is 1 if the pump is working and 0 conversely. In fact, the reliability of the distribution network requires using two pumps for each pipe and thus the indexes a and b will indicate this redundancy. Actually, the pump outflows are constant, thus, by comparing the outflows with the corresponding working states, residuals can be generated. In the case of the pumping station "Haut de Blemont", four models can be formulated. Their expressions are the following:

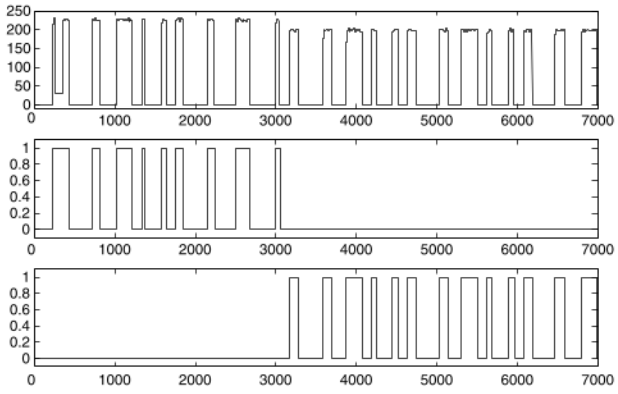

Fig. 11. Flow-rate signal $q_{35}(k)$ and working state signal $w_{a,35}(k)$ and $w_{b,35}(k)$.

$$q_{35}(k) = w_{a,35}(k)\bar{q}_{a,35} + w_{b,35}(k)\bar{q}_{b,35} \quad (31a)$$

$$q_{36}(k) = w_{a,36}(k)\bar{q}_{a,36} + w_{b,36}(k)\bar{q}_{b,36} \quad (31b)$$

$$q_{38}(k) = w_{a,38}(k)\bar{q}_{a,38} + w_{b,38}(k)\bar{q}_{b,38} \quad (31c)$$

$$q_{38b}(k) = w_{a,38}(k)\bar{q}_{a,38b} + w_{b,38}(k)\bar{q}_{b,38b} \quad (31d)$$

where $\bar{q}_{a,i}$ and $\bar{q}_{b,i}$ represent an estimation of the mean value of outflow q_i delivered by each pump. Using validated data, a least square approach has been used to estimate the parameters of these models: $\bar{q}_{a,35} = 142.95$ and $\bar{q}_{b,35} = 148.18$, $\bar{q}_{a,36} = 115.20$ and $\bar{q}_{b,36} = 114.49$, $\bar{q}_{a,38} = 225.70$ and $\bar{q}_{b,38} = 199.50$, $\bar{q}_{a,38b} = 213.31$ and $\bar{q}_{b,38b} = 159.27$.

Thus models (31) will be used further for generating residuals based on the available measurements. These residuals are particularly interesting for the detection of pump dysfunction.

4.2.3. Relations between flow-rate and pressure measurements

The flow-rate q_{44} supplies a residential area in which two sensors give the evolution of pressures called p_7 and p_8. According to hydraulic laws, a link between flow-rate q_{44} and pressures p_7 and p_8 is expected. That has been confirmed by a statistical analysis of the measurements, which has put into relief the existence of a clear correlation between q_{44}, p_7 and p_8. The values of the corresponding correlation coefficients are given in Table 7.

Consequently, some models linking these measurements have been established by carrying out a parameter estimation. The models defined by expression (32), which enables to compute an estimation of flow-rate q_{44} from measurements p_7, p_8, q_{39} and q_{42}, have finally been selected:

$$q_{44} = -95.2\tanh\frac{p_7 - 7000}{800} - 172.09\tanh\frac{p_8 - 3500}{800} + 74.16 \quad (32a)$$

Table 7
Values of the correlation coefficients

	q_{39}	q_{40}	q_{41}	q_{42}	q_{44}
p_7	−0.55	−0.40	−0.35	−0.36	−0.64
p_8	−0.67	−0.52	−0.46	−0.47	−0.80

$$q_{44} = -18.82p_7 - 187.63p_8 + 1.141q_{39} + 0.240q_{42} + 914.13 \quad (32b)$$

The estimation of flow-rate q_{44} obtained by using model (32a) is illustrated by Fig. 12. This figure represents the results obtained with validation data. The modeling data used for the parameter estimation recover a period of 13,000 samples, which correspond to about 9 days. The correlation coefficient between the measurement and estimation of q_{44}, obtained with validated data, is equal to 0.85; thus the obtained model explains not perfectly but satisfactorily the flow-rate q_{44} and as indicated by Fig. 12 low flow-rates are sometimes poorly estimated. From that model a residual can be evaluated by comparing the measurement of q_{44} and its estimation.

4.2.4. Relations between flow-rate measurements

The analysis of the flow-rate signals has put into relief the fact that the water consumptions of some residential areas are very similar. For instance, flow-rates q_{39} and q_{44} (Fig. 10), which supply distinct areas have the same cyclic shape. This shape is characteristic of the consumption habits of the inhabitants. In the case of the pumping station "Haut de Blemont", the flow-rates q_{39}, q_{40}, q_{41}, q_{42} and q_{44} supply residential areas. The correlation analysis of these measurements (Table 8) confirms that there is quite a clear similarity between these measurements.

Consequently, empirical relations linking these variables have been established by carrying out a parametric estimation. As an example, relations (33) enable to compute an estimation of flow-rates q_{39}, q_{40}, q_{41} and q_{44} by using some

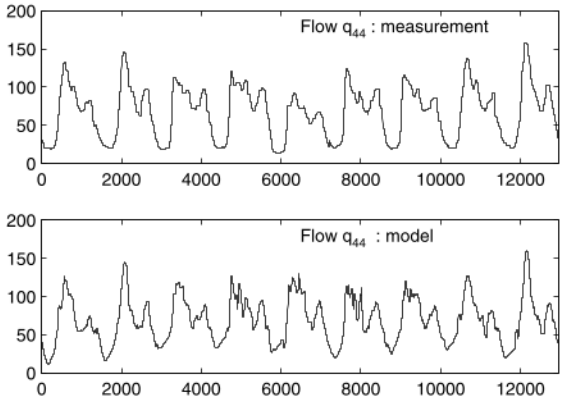

Fig. 12. Estimation of flow-rate q_{44}.

Table 8
Values of the correlation coefficients for the flow-rates

	q_{39}	q_{40}	q_{41}	q_{42}	q_{44}
q_{39}	1.00	0.62	0.59	0.61	0.84
q_{40}	0.62	1.00	0.71	0.71	0.62
q_{41}	0.59	0.70	1.00	0.98	0.62
q_{42}	0.61	0.71	0.98	1.00	0.63
q_{44}	0.84	0.62	0.62	0.63	1.00

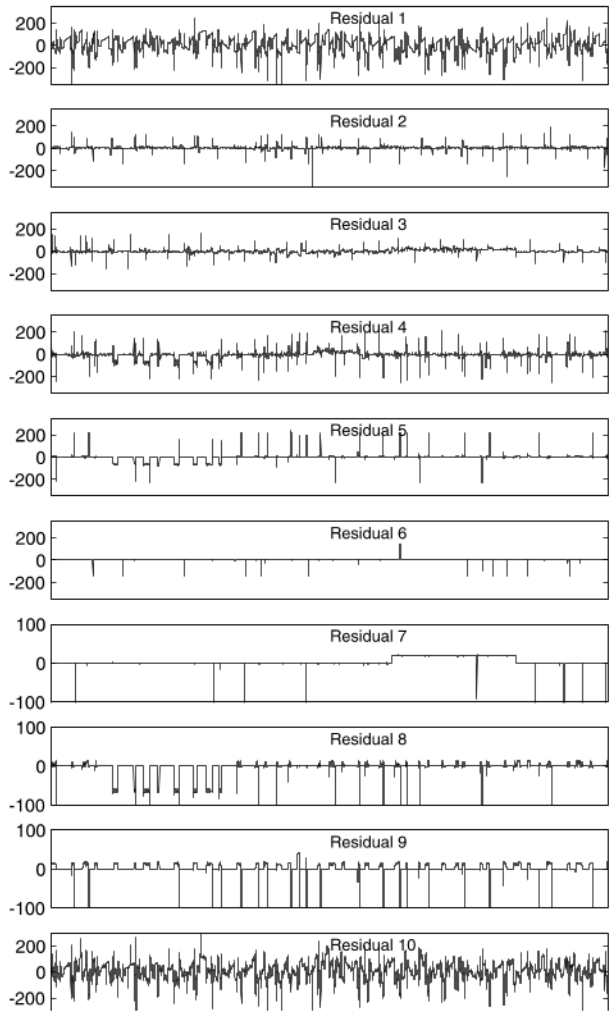

Fig. 13. Experimental residuals $r_1(k)$ to $r_{10}(k)$.

of the measurements of these flow-rates (no satisfactory model has been obtained for flow-rate q_{42}. The results obtained with this relation show that the proposed models allow to give a good prediction of the flow-rates. For example, the correlation between the estimation of flow-rate q_{44} and its measurement is equal to 0.96 which indicates a good explanation of the corresponding model:

$$q_{39} = 0.155q_{40} + 0.357q_{44} + 4.774 \quad (33a)$$

$$q_{40} = 0.134q_{39} + 0.090q_{41} + 3.903 \quad (33b)$$

$$q_{41} = 2.834q_{42} - 1.963 \quad (33c)$$

$$q_{44} = 2.124q_{39} + 0.592q_{40} - 0.934 \quad (33d)$$

4.3. Residual generation

Thus, models (29)–(33) allow to generate residuals; these residuals can be evaluated from experimental data and are drawn in Fig. 13. To sum up, 38 redundancy relations have been established: – 5 material balance equations – 4 relations using pump working states – 3 relations between pressures and flow-rate – 26 relations linking flow rates.

For the sake of simplicity, only some of the models have been previously given. The kinds of faults which can be detected or isolated by using this residuals are: flow-rate measurement faults, pressure measurement faults, leaks or pipes breakages and pumps or gates dysfunctions.

In the following, only examples are given for flow-rate measurement faults.

4.4. Examples of real faults isolation

Let us now show how the proposed approach enables to isolate faults. The residuals appearing in Fig. 13 have been computed by using experimental data. A period of 13,000 min, which represent about 9 days, is considered here. During this period, a visual inspection of the graphs clearly shows that the residuals r_5 and r_8 are affected by a fault from time 4 to time 6 and residual r_7 from time 8.5 to time 10.5 (2 days); some other residuals are also affected but the scale of the graphs and the presence of random variations do not allow a clear analysis.

To go further in the diagnosis, expressions (34) give the structure of the residuals obtained from the models; indeed

Table 9
Occurrences of variables in residuals

	h_4	h_{18}	h_{19}	h_{21}	q_3	q_{35}	q_{36}	q_{38}	q_{38b}	q_{39}	q_{40}	q_{41}	q_{42}	q_{44}	w_{35}	w_{36}	w_{38}	p_7	p_8
1	X	·	·	·	X	X	X	X	·	·	·	·	·	·	·	·	·	·	·
2	·	X	·	·	·	X	·	·	·	X	X	·	·	·	·	·	·	·	·
3	·	·	X	·	·	·	X	·	·	·	·	X	X	·	·	·	·	·	·
4	·	·	·	X	·	·	·	X	·	·	·	·	·	X	·	·	·	·	·
5	·	·	·	·	·	·	·	X	X	·	·	·	·	·	·	·	·	·	·
6	·	·	·	·	·	X	·	·	·	·	·	·	·	·	X	·	·	·	·
7	·	·	·	·	·	·	X	·	·	·	·	·	·	·	·	X	·	·	·
8	·	·	·	·	·	·	·	X	·	·	·	·	·	·	·	·	X	·	·
9	·	·	·	·	·	·	·	·	X	·	·	·	·	·	·	·	X	·	·
10	X	X	X	X	X	·	·	·	·	X	X	X	X	X	·	·	·	·	·
11	·	·	·	·	·	·	·	·	·	·	·	·	·	X	·	·	·	X	X
12	·	·	·	·	·	·	·	·	·	X	·	·	X	X	·	·	·	X	X
13	·	·	·	·	·	·	·	·	·	X	X	·	·	X	·	·	·	·	·
14	·	·	·	·	·	·	·	·	·	X	X	X	·	·	·	·	·	·	·
15	·	·	·	·	·	·	·	·	·	·	·	X	X	·	·	·	·	·	·
16	·	·	·	·	·	·	·	·	·	X	X	·	·	X	·	·	·	·	·

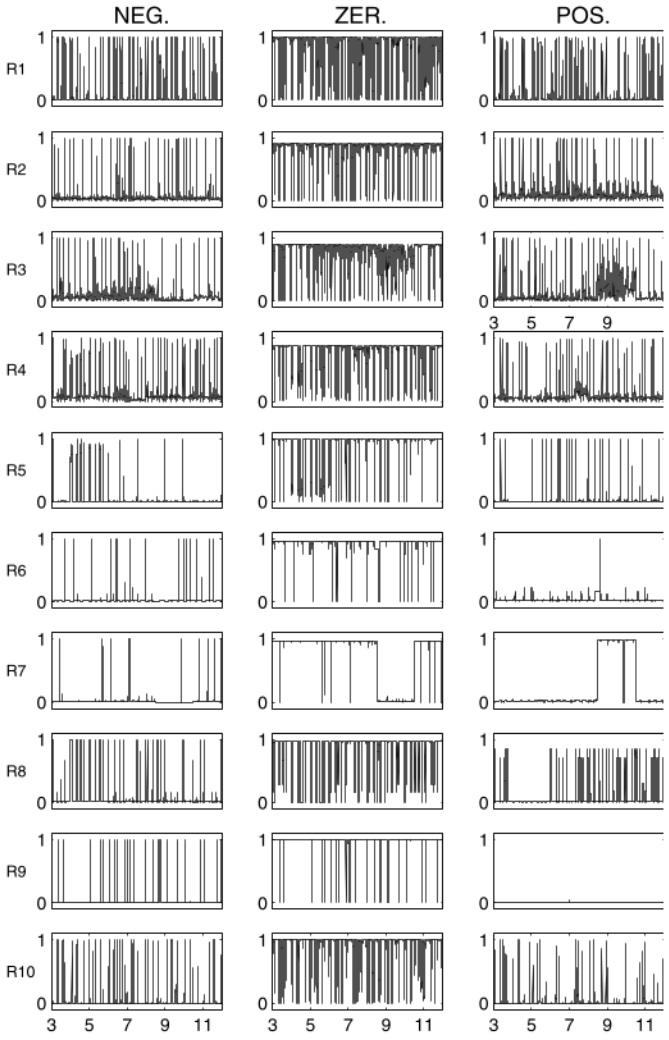

Fig. 14. Truth values of the residuals r_1 to r_8.

only the occurrences of the variables (Table 9) which intervene in each residual have been mentioned:

$$r_1 = f(h_4, q_3, q_{35}, q_{36}, q_{38}) \tag{34a}$$
$$r_2 = f(h_{18}, q_{35}, q_{39}, q_{40}) \tag{34b}$$
$$r_3 = f(h_{19}, q_{36}, q_{41}, q_{42}) \tag{34c}$$
$$r_4 = f(h_{21}, q_{38}, q_{44}) \tag{34d}$$
$$r_5 = f(q_{38}, q_{38b}) \tag{34e}$$
$$r_6 = f(q_{35}, w_{a,35}, w_{b,35}) \tag{34f}$$
$$r_7 = f(q_{36}, w_{a,36}, w_{b,36}) \tag{34g}$$
$$r_8 = f(q_{38}, w_{a,38}, w_{b,38}) \tag{34h}$$
$$r_9 = f(q_{38b}, w_{a,38}, w_{b,38}) \tag{34i}$$
$$r_{10} = f(h_4, h_{18}, h_{19}, h_{21}, q_3, q_{39}, q_{40}, q_{41}, q_{42}, q_{44}) \tag{34j}$$
$$r_{11} = f(q_{44}, p_7, p_8) \tag{34k}$$
$$r_{12} = f(q_{44}, p_7, p_8, q_{39}, q_{42}) \tag{34l}$$
$$r_{13} = f(q_{39}, q_{40}, q_{44}) \tag{34m}$$
$$r_{14} = f(q_{40}, q_{39}, q_{41}) \tag{34n}$$
$$r_{15} = f(q_{41}, q_{42}) \tag{34o}$$
$$r_{16} = f(q_{39}, q_{40}, q_{44}) \tag{34p}$$

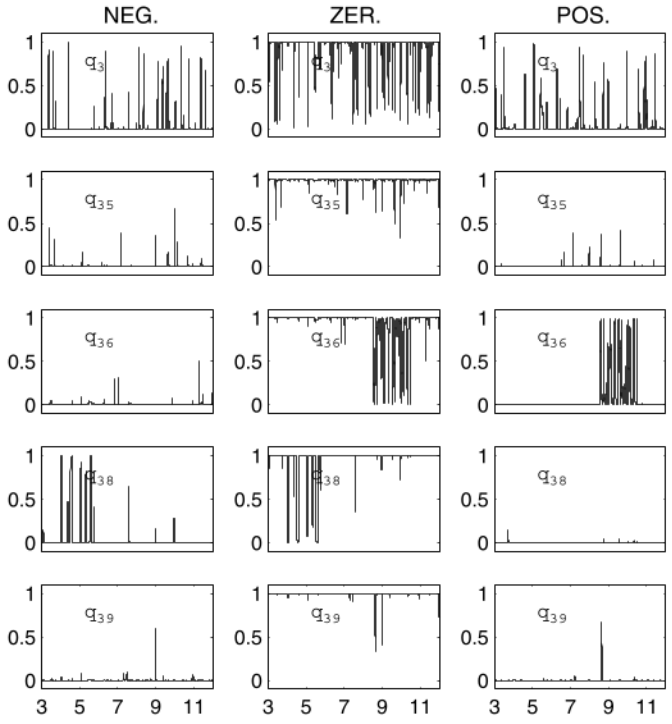

Fig. 15. Truth values of failure hypothesis f_3^-, f_3^+, f_{35}^-, f_{35}^+, f_{36}^-, f_{36}^+, f_{38}^-, f_{38}^+, f_{39}^- and f_{39}^+ without taking into account the residuals sensitivity.

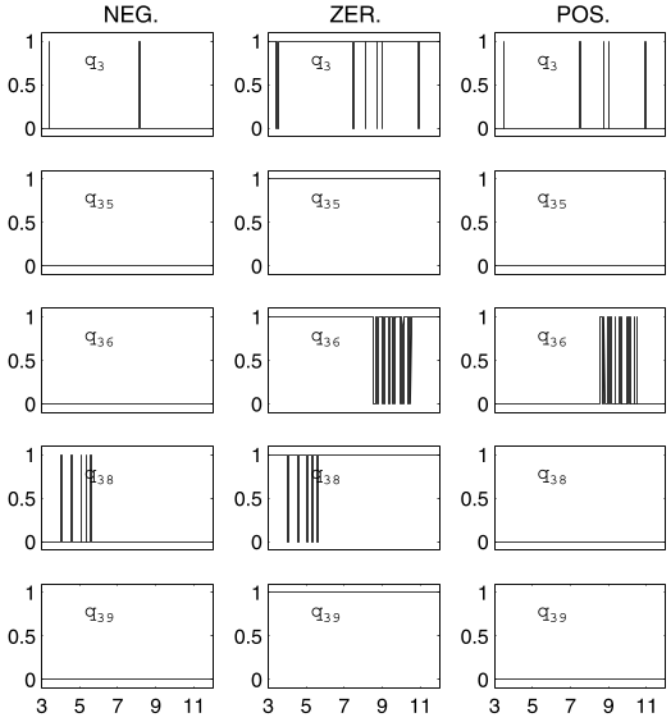

Fig. 16. Truth values of failure hypothesis f_3^-, f_3^+, f_{35}^-, f_{35}^+, f_{36}^-, f_{36}^+, f_{38}^-, f_{38}^+, f_{39}^- and f_{39}^+ by taking into account the residuals sensitivity.

The fuzzy-based fault isolation procedure is based on the analysis of the 16 residuals (Fig. 14). The fault

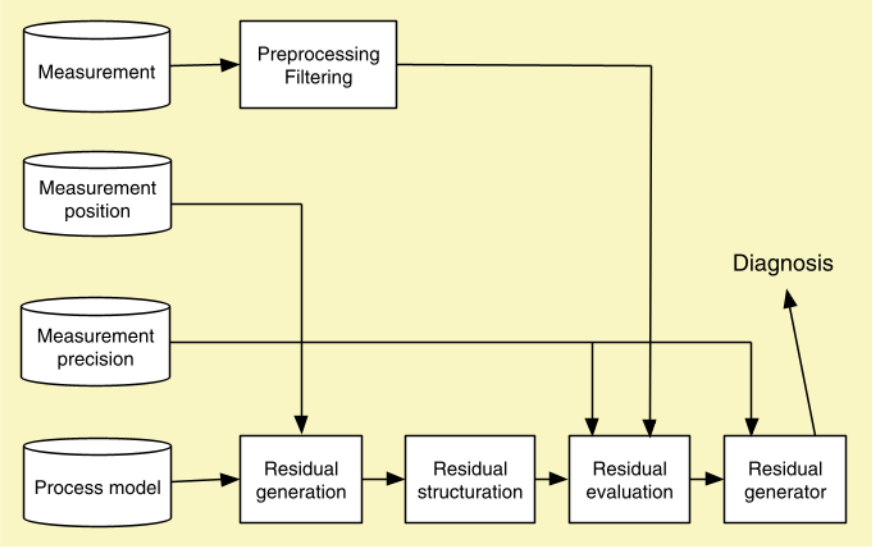

Fig. 17. Diagnosis procedure.

hypothesis corresponding to negative (resp. positive) faults affecting q_{36}, q_{38} and q_{44} are respectively written f_{36} (resp. f_{36}^{+}), f_{38} (resp. f_{38}^{+}) and f_{44} (resp. f_{44}^{+}). The results of the systematic fault isolation procedure, without taking into account the sensitivity appear in Fig. 15. Referring to this figure the most likely fault hypothesis is f_{36}^{+}, which corresponds to a positive fault affecting flow-rate q_{36}. By taking into account the sensitivity of the residuals (Section 3.2.3), the fault isolation results (Fig. 16) are clearly improved. According to these results the failure hypothesis f_{36}^{+} can now undoubtedly be designated as the most likely. The observation of flow-rate q_{38} during the same period (Fig. 16) confirms that it has been affected by a fault from time 4424 to time 5172.

4.5. Implementation of the fault isolation procedure

The proposed fault isolation procedure is described by Fig. 17. First of all a data processing stage is necessary, to eliminate the outlier and filter the measurement noises. Then, by using the filtered data and the redundancy relations presented previously residuals can be generated. On the basis of these residuals, the fuzzy-based isolation method enables to find out the most likely fault hypothesis. The results are submitted to human operators who can, on the basis of their knowledge of the process or additional information, confirm or invalidate these results in order to propose a diagnosis.

This procedure has been integrated to the supervision system of the water supply network. The results of the fault isolation method are offered to the human operators under a synthetic form. The diagram of the supervised part of the network is displayed on the supervision screens and the results are presented on this diagram. They are translated by using a color code progressively going from green to red. Low truth values of the fault isolation hypothesis appear in green and high truth values are represented in red.

5. Conclusion

The purpose of this study is to develop a method to identify the location of faulty sensors in a water distribution delivery system by monitoring the flow-rate. In the paper a fault isolation method based on fuzzy concepts is applied to a water supply network. The efficiency of the suggested method has been proved by the results obtained with experimental data. Consequently, a supervision software has been developed on the basis of this approach. The use of fuzzy concepts enables to easily take advantage of all the available data and knowledge. Besides, fuzzy reasoning is particularly adapted to the case of uncertain data or models. These aspects contribute strongly to the improvement of the supervision efficiency. This study is very fruitful because it has put into relief the difficulties linked to the implementation of a supervision procedure for a real process. Furthermore, from a theoretical point of view, this application has revealed the limits of the existing methods and forced us to propose some improvements. So, some concepts, specific to fault isolation have been introduced. An aggregation operator particularly adapted to the problem of fault isolation has been defined. Moreover, additional indicators are proposed in order to take into account the temporal persistence of the symptoms, the confidence attached to the redundancy relations or the sensitivity of the residuals. An analysis of various fault situations revealed that in the case of a real process there exists a high proportion of simultaneous faults. Unfortunately these situations are very difficult to handle, that is why further research on this aspect will be required in the near future.

References

[1] J. Armengol, J. Vehi, M. Sainz, P. Herrera, Fault detection in a pilot plant using interval models and multiple sliding time windows, in: Proceedings of the Fifth IFAC Symposium on Fault Detection, Supervision and Safety of Technical Processes, Safeprocess 2003, Washington, DC, USA, June 2003, pp. 729–734.

[2] J.H. Andersen, R.S. Powell, J.F. Marsh, Constrained state estimation with applications in water distribution network monitoring, International Journal of Systems Science 32 (6) (2001) 807–816.

[3] W. Berry, Sensor placement in municipal water networks, Journal of Water Resources Planning and Management 131 (3) (2005) 237–243.

[4] M. Blanke, M. Kinnaert, J. Lunze, M. Staroswiecki, Diagnosis and Fault-Tolerant Control, Springer, 2003.

[5] B. Bouchon-Meunier, La logique floue et ses applications, Collection Vie Artificielle, Addison-Wesley, Paris, 1995.

[6] C. Bragalli, D.A. Savic, E. Keedwell, S. Arting, Multiple objectives and water quality in water distribution networks, in: Cabrera, Cabrera Jr. (Eds.), Pumps, Electromechanical Devices and Systems Applied to Urban Water Management, 2003, pp. 27–35.

[7] P. Carpentier, G. Cohen, State estimation and leak detection in water distribution networks, Civil Engineering Systems 8 (1992) 247–257.

[8] P. Carpentier, G. Cohen, State estimation and leak detection in water distribution networks, French–UK Workshop in Operational Control of Water Distribution Networks, Heriot-Watt University, Edinburgh, 3–5 April 1991.

[9] E.Y. Chow, A.S. Willsky, Analytical redundancy and the design of robust failure detection system, IEEE Transactions on Automatic Control AC-29 (7) (1984) 603–614.

[10] H.J. Convey, M.J. Booth, Development of a water leak detection system, Computing and Control Engineering Journal (February) (2002).

[11] R. Farmani, D.A. Savic, G.A. Walters, Evolutionary multi-objective optimisation in water distribution network design, Engineering Optimisation 37 (2) (2005) 167–183.

[12] P.M. Frank, Analytical and qualitative model-based fault diagnosis – a survey and some new results, European Journal of Control 2 (1) (1996) 6–28.

[13] B. Gabrys, A. Bargiela, Neural simulation of water systems for efficient state estimation, in: M. Snorek, M. Sujansky, A. Verbraeck (Eds.), Proceedings of Modelling and Simulation Conference ESM'95, Prague, 1995, pp. 775–779.

[14] B. Gabrys, A. Bargiela, Integrated neural based system for state estimation and confidence limit analysis in water networks, in: Proceedings of European Simulation Symposium ESS'96, Genoa, 2, 1996, pp. 398–402.

[15] J. Gertler, Survey of model-based failure detection and isolation in complex plants, IEEE Control Systems Magazine 8 (6) (1988) 3–11.

[16] J. Gertler, K.C. Anderson, An evidential reasoning extension to quantitative model-based failure diagnosis, IEEE Transactions on Systems, Man and Cybernetics 22 (2) (1992) 275–289.

[17] J. Gertler, Analytical redundancy methods in fault detection and isolation – survey and synthesis, in: IFAC Symposium Safeprocess'91, Baden-Baden, 1991, pp. 9–21.

[18] I. Gupta, A. Gupta, P. Khanna, Genetic algorithm for optimisation of water distribution systems, Environmental Modelling and Software 14 (5) (1999) 437–446.

[19] G.D. Hainsworth, Measurement uncertainty in water distribution telemetry systems, PhD Thesis, Trent Polytechnic, Nottingham, UK, 1988.

[20] R.D. Carr, H.J. Greenberg, W.E. Hart, C.A. Phillip, Addressing Modeling Uncertainties in Sensor Placement for Community Water Systems, 2004.

[21] R. Isermann, Process fault detection based on modeling and estimation methods: a survey, Automatica 20 (4) (1984) 387–404.

[22] Z. Kapelan, D. Savic, G. Walters, D. Covas, N. Graham, C. Maksimovic, An assessment of the application of inverse transient analysis for leak detection: Part 1 – theoretical considerations, Computer Control for Water Industry (2003).

[23] Z. Kapelan, A.V. Babayan, D.A. Savic, G.A. Walters, S.T. Khu, Two new approaches for the stochastic least cost design of water distribution system, Water Supply 4 (5–6) (2005) 355–363.

[24] M.A. Kramer, Malfunction diagnosis using quantitative models with non-Boolean reasoning in expert systems, AICHE Journal 33 (1) (1987) 130–140.

[25] Ryan M. Lesyshen, Water transmission line leak detection using extended Kalman filtering, Master of Science, University of Saskatchewan, 2005. Available from: <http://library.usask.ca/theses/available/etd-03242005-110841>.

[26] D. Mandel, Diagnostic ábase de redondance analytique. Application á un réseau urbain de distribution d'eau potable, Doctorat de l'Institut National Polytechnique de Lorraine, Nancy, France, 1988.

[27] S. Narasimhan, C. Jordache, Data Reconciliation and Gross Error Detection, Gulf Publishing Company, Houston, Texas, 2000.

[28] B. Nguyen, Accuracy in water losses estimation in the distribution network – the Paris case, Water Supply 4 (3) (2004) 123–132.

[29] M. Nyberg, M. Krysander, Combining AI, FDI, and statistical hypothesis-testing in a framework for diagnosis, Presented at the Bridge Day at SafeProcess, DX 03, in: Proceedings of the Fifth IFAC Symposium on Fault Detection, Supervision and Safety of Technical Processes, Safeprocess 2003. Washington, DC, USA, June 2003, pp. 891–896.

[30] D.B. Özyurt, Ralph W. Pike, Theory and practice of simultaneous data reconciliation and gross error detection for chemical processes, Computers and Chemical Engineering 28 (2004) 381–402.

[31] T.F. Petti, J. Klein, P.S. Dhurjati, Diagnostic model processor: using deep knowledge for process fault diagnosis, AICHE Journal 36 (4) (1990) 565–575.

[32] J. Romagnoli, M. Sanchez, Data Processing and Reconciliation for Chemical Process, Academic Press, 2000.

[33] M. Shinozuka, J. Liang, Q. Feng, Detection of damage location and extent of water supply systems, in: Proceedings of Workshop on Mitigation of Earthquake Disaster by Advanced Technologies, March 2–3, Los Angeles, pp. 55–61.

[34] S. Simani, C. Fantuzzi, R. Patton, A Model-based Fault Diagnosis in Dynamic Systems using Identification Techniques, Springer, 2002.

[35] F. Bessler, D.A. Savic, G.A. Walters, Water reservoir control with data mining, ASCE Journal of Water Resources Planning and Management 129 (1) (2003) 26–34.

[36] R. Farmani, D.A. Savic, G.A. Walters, Benchmark problems for design and optimization of water distribution systems, in: Maksimovic, Butler, Memon (Eds.), Advances in Water Supply Management, 2003, pp. 249–256.

[37] T.G. Watson, C.D. Christian, A.J. Mason, M.H. Smith, R. Meyer, Bayesian-based pipe failure model, Journal of Hydroinformatics 6 (2004) 259–264.